Charles University Prague
Faculty of Mathematics and Physics

BACHELOR THESIS

Tomáš Kosek

Jet modification in heavy ion collisions

Institute of Particle and Nuclear Physics

Supervisor: RNDr. Jiří Dolejší, CSc.
Study programme: General Physics

2007

Univerzita Karlova v Praze
Matematicko-fyzikální fakulta

BAKALÁŘSKÁ PRÁCE

Tomáš Kosek

Ovlivnění jetů ve srážkách těžkých iontů

Ústav částicové a jaderné fyziky

Vedoucí bakalářské práce: RNDr. Jiří Dolejší, CSc.
Studijní program: Obecná fyzika

2007

I would like to thank to my supervisor Jiří Dolejší who explained me some difficult terms both in theoretical and experimental physics. My thanks belong also to my classmate Martin Rybář for his comments and discussions about jet physics.

I declare that I wrote my bachelor thesis independently and exclusively with the use of the cited sources. I agree with lending and publishing the thesis.

Prohlašuji, že jsem svou bakalářskou práci napsal samostatně a výhradně s použitím citovaných pramenů. Souhlasím se zapůjčováním práce a jejím zveřejňováním.

In Prague, 10^{th} August 2007 Tomáš Kosek

Contents

Název práce: Ovlivnění jetů ve srážkách těžkých iontů
Autor: Tomáš Kosek
Katedra (ústav): Ústav částicové a jaderné fyziky
Vedoucí bakalářské práce: RNDr. Jiří Dolejší, CSc.
e-mail vedoucího: jiri.dolejsi@mff.cuni.cz

Abstrakt: V této práci jsou uvedeny některé experimentální výsledky získané na urychlovači RHIC v BNL, které ukazují na podstatné změny ve vlastnostech jetů vzniklých ve vysokoenergetické srážce dvou těžkých jader ve srovnání s jety vzniklými ve srážce dvou protonů. Tyto změny se projevují ve snížené produkci hadronů s velkou příčnou hybností a ve změně tvaru jetů jejichž mateřský parton prolétl jadernou hmotou vzniklou po srážce. Studiem výše zmíněných změn jsou zjišťovány vlastnosti této hmoty a možnost vzniku kvark gluonového plazmatu

Klíčová slova: ovlivnění jetů, srážky těžkých iontů, kvark gluonové plasma

Title: Jet modification in heavy ion collisions
Author: Tomáš Kosek
Department: Institue of Particle and Nuclear Physics
Supervisor: RNDr. Jiří Dolejší, CSc.
Supervisor's e-mail address: jiri.dolejsi@mff.cuni.cz

Abstract: In this bachelor thesis some of the experimental results from RHIC at BNL are reviewed. These results show significant changes in properties of jets created after the ultra-relativistic heavy ion collision relative to jets created by the proton-proton collision. These changes are manifested in the large suppression of the high transverse momentum hadrons, and in the shape changes of the jet whose mother-parton traversed through the nuclear matter created after the collision. Properties of this matter and possibility of the quark-gluon plasma creation are studied via above mentioned changes.

Keywords: jet quenching, heavy ion collisions, quark-gluon plasma

Chapter 1

Introduction

In the latter half of the twentieth century the theory of strong interaction, quantum chromodynamics (QCD), was developed to describe physics of strong interaction. It is quantum field theory. QED describes electromagnetic interaction, *i. e.*, interaction between electrically charged particles (electrons, protons,...). They interact with each other by the exchange of massless, uncharged particles, photons. Analogously to QED, in QCD interact color charged particles called quarks. There are six quarks, which differ in mass and flavor, and six antiquarks with oposite charges. Quarks interact with each other by the exchange of gluons, which are, analogous to photons, massles spin-1 particles with no electric charge but with non zero color charge. Quarks and gluons interact much strongly than photons and fermions in QED what makes QCD much harder to analyze than QED.

QCD has two fundamental, at first glance contradictory properties:
asymtotic freedom: strong interaction becomes weaker if momentum transfer in studied processes is large
confinement of quarks (or just confinement): There has never been observed isolated color charged particle (quark). All quarks are confined into pairs (mesons) or triplets (baryons) so that the color charge of the combination is zero. There is no obvious mathematical reason for confinement.

The QCD Langrangian is known for a long time but relevant properties are not calculable (structure of baryons, cross section of low p_T production reactions,...). There are two main methods how to exceed this problem. First method is perturbation QCD (PQCD). The gluon screening effectively increases the strong's force coupling constant α_s (analog to fine structure constant α), but this constant depends on the momentum transfer Q^2. This

means that in high energy experiments, where is large momentum transfer, is gluon screening less effective and we can use perturbation calculation. The second method is lattice QCD (LQCD). It is numerical method which uses discrete space-time lattice to calculate observables of the studied system. LQCD can be used to solve low energetic problems, also the quark confinement can be easily demonstrated with LQCD.

One particular area that QCD should describe is nuclear matter under extreme conditions. We are interested in extremely high temperature and energy density because it is predicted that hadronic matter heated to extremely high temperature will cause hadrons to "melt" and deconfine partons, *i. e.*, quarks and gluons. This partonic matter is called Quark-Gluon Plasma (QGP), considered [1] (direct citations are in quotes and typed by *italic*) *"as a (locally) thermally equilibrated state of matter in which quarks and gluons are deconfined from hadrons, so that color degrees of freedom become manifest over nuclear, rather than merely nucleonic volumes."* Physicists intensively study QGP because they hope that research of QGP will help to better understanding of color confinement or QCD at all. The research of QGP is interesting also from astrophysical point of view because it is generally thought that a few microseconds after big bang the universe was in QGP state until its energy density decreased and the transition into hadrons started.

Chapter 2

QGP and jet quenching

2.0.1 Transition between hadronic matter and QGP

"The predicted transition from ordinary nuclear matter, which consists of hadrons inside which quarks and gluons are confined, to QGP, a state of matter in which quarks and gluons are no longer confined to volumes of hadronic dimensions, can in the simplest approach, be likened to the transition between two thermodynamic states in a closed volume." [2]

It is predicted by LQCD that critical temperature for Quark-Gluon Plasma formation is $T_C \approx 170$ MeV $\approx 10^{12}$ K. Graphical representation of LQCD results is in figure 1. This transition temperature corresponds to an energy density $\epsilon \approx 1$ Gev/fm^3. [3]

The order of phase transition is not known. If only gluons are considered the transition appears to be first order. The order of transition will change if two light quarks (up and down) or three quarks (up, down and strange quark) are considered [3]. Then first order transition change to second order transition. These results are obtained only if net baryon density is zero. The schematic phase diagram is in figure 2. There is tricritical point in phase diagram - for lower values of chemical baryon density μ the transition is second order while for higher values it is first order transition. One can also see that with increasing chemical baryon density decreases critical temperature T_C.

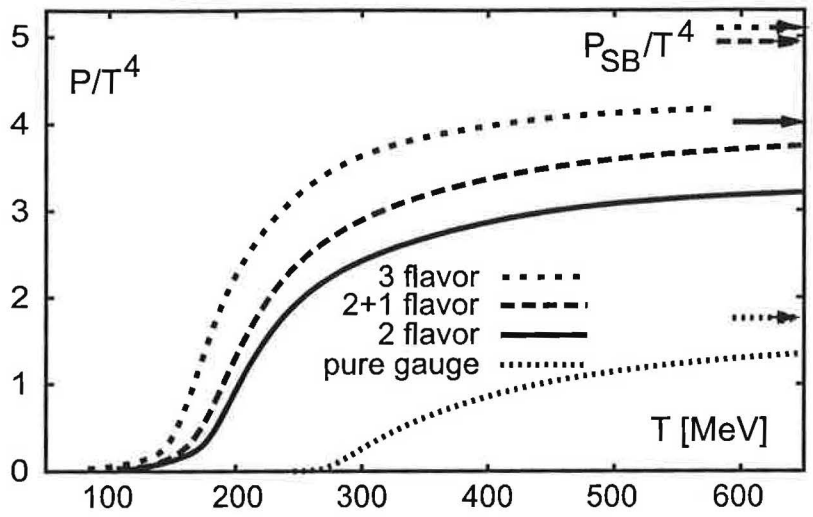

Figure 2.1: LQCD results for the pressure/T^4 dependence on T for different choices of the number of quark flavors. Arrows on the right axis indicate Stefan-Boltzmann limits for corresponding flavor assumptions. Figure taken from [1]

2.1 QGP and Heavy-Ion Collisions

About 30 years ago has been conjectured that a QGP phase could be created by colliding two heavy nuclei. Schematic picture of the time and energy density scales is in figure 3. First experimental attempts to create QGP in the laboratory were done at Berkeley BEVALAC in 1984 (center of mass energies per nucleon pair were $\sqrt{s_{NN}} \approx 1$ GeV) followed by AGS at Brookhaven National Laboratory ($\sqrt{s_{NN}} = 5$ GeV) and SPS accelerator at CERN ($\sqrt{s_{NN}} = 17$ GeV). No final proof of QGP formation was found in the experiments at those energies but results from SPS provided evidence for possible formation of QGP.

The Relativistic Heavy Ion Collider (RHIC) at Brookhaven National Laboratory provides the most energetic beams of heavy ions now available (for more information about RHIC and its experiments see APENDIX A). At RHIC the maximal beam energy of colliding beams is 100 GeV per nucleon, so $\sqrt{s_{NN}} = 200$ GeV the center of mass energy in central collisions between gold nuclei is almost 40 TeV. A significant fraction of this energy is converted

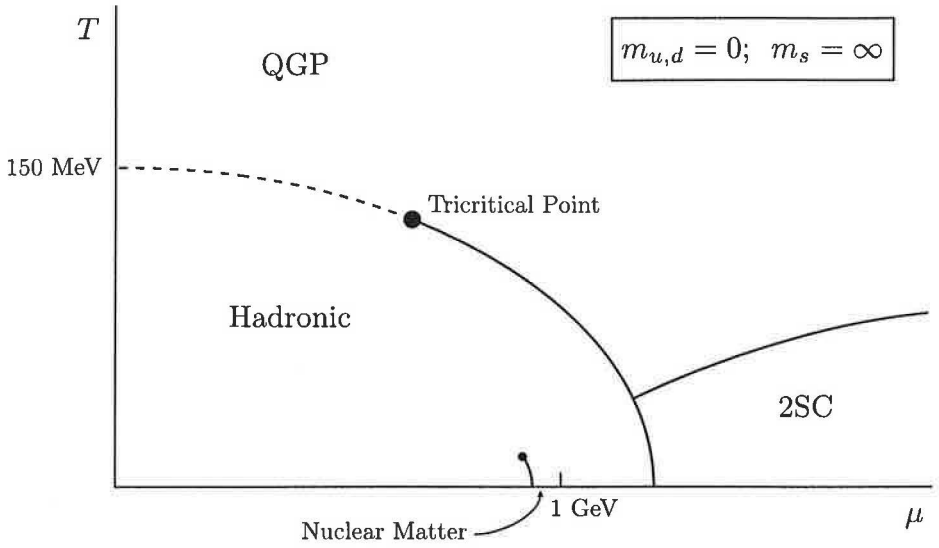

Figure 2.2: Theoretical phase diagram of nuclear matter for two massless quarks as a function of temperature T and baryon chemical potential μ. 2SR region is the color superconducting phase of matter. Figure taken from [3]

into matter - many thousands of particles are created in the limited volume what produces the energy density needed for QGP creation. It is estimated that energy density for central Au collisions at RHIC ($\sqrt{s_{NN}} = 200$ GeV) is more than 5 GeV/fm^3

It is evident, that existence of such hot and dense matter gives the big chance to observe signatures of QGP. Generally there are two types of signatures [1, 3, 2]:

- the bulk thermodynamic properties such as large energy density, entropy growth, collective flow, correlations among the soft hadrons, etc.
- specific properties of particles which interact with a QGP, *i. e.*, modification of widths and masses of resonances, modification of particle production probabilities due to color screening and modification of parton properties due to interaction with the dense medium, the so called *jet quenching.*

We are interested in the last mentioned phenomenon, jet quenching. In next sections, after very brief introduction into the mechanisms of jet

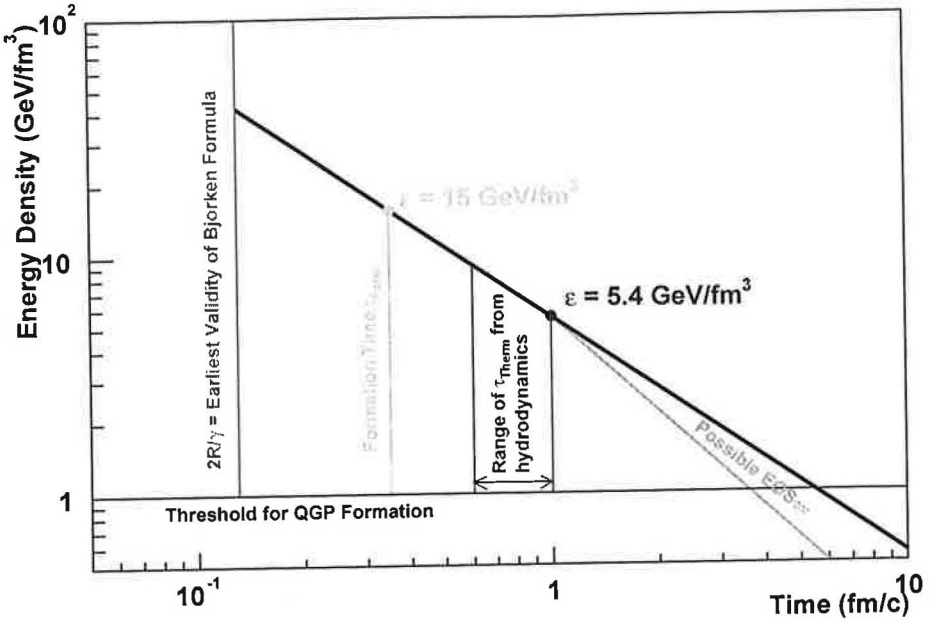

Figure 2.3: Time and energy density scales. Figure taken from [3]

quenching we review the experimental results from RHIC which show the jet quenching and stimulated another intensive research.

Chapter 3

Propagation of partons throughout the dense QCD media

3.1 Energy loss

High p_T partons propagating through the dense QCD matter created in a heavy ion collision, are expected to lose a significant part of it's energy. There are two possible ways how particle can loose its energy by propagating throughout the medium - either it looses energy by colliding with the medium's particles or by radiating massles particles. It is thought that accordingly to QED, where charged particles propagating through the medium emit brehmstrahlung photons taking an energy ΔE away, also in QCD partons emit bremstrahlung gluons. However, some physicists thought that energy loss is caused by colliding mechanism [4].

The measured energy loss can be linked to thermodynamical or transport medium properties. If these properties can be computed or estimated, than we can compare theoretical predicted values with measured ones. One of the properties which are frequently appearing in the literature [5] is transport coeficient $\langle \hat{q} \rangle$ which characterizes the squared average momentum transfer from medium to hard parton per unit distance. Energy loss ΔE dependence on $\langle \hat{q} \rangle$ is:

$$\langle \Delta E \rangle \propto \alpha_s C_R \langle \hat{q} \rangle L^2 \tag{3.1}$$

where L is the lenght traversed by the parton in medium.

3.2 Modified dihadron azimuthal correlations

A fast parton traversing medium undergoes multiple scattering. During this interactions it acquires additional transverse momentum to its original direction and in conjuction with energy loss it leads to what is called jet broadening.

Another class of interesting observables could be dijet correlations. Extreme example is production of dijet on the surface of the medium with one parton traversing through the matter (and forming jet greatly influenced by the medium) and the other parton directed into the vacuum and creating jet like in hadron collision.

Chapter 4

Suppression of high p_T hadrons

4.1 Introduction

The simple way to study properties of nucleus - nucleus (NN) collisions is to compare them with proton - proton collisions which are simpler and better understood. The high momentum transfer processes are induced via relatively short-range interactions. Thus it is expected that particular hard processes can be induced by binary collisions in the overall nucleus-nucleus interaction [6].

If two nuclei collide with non zero impact parametr $\mathbf{b}$ a nucleus sees a slab of nuclear matter of the thickness (z is measured along the beam) [7]:

$$T_A(\mathbf{b}) = A \int_{-\infty}^{\infty} \rho_A(\mathbf{b}, z) \tag{4.1}$$

where $\rho_A(\mathbf{b}, z)$ is nucleon density distribution. Then nuclear overlap function then can be expressed as:

$$T_{AA}(\mathbf{b}) = \int T_A(\mathbf{s}) T_A(\mathbf{b} - \mathbf{s}) d^2\mathbf{s} \tag{4.2}$$

If NN collision isn't infuenced by other processes then it should be enhanced by T_{AA} factor. In other words, T_{AA} expresses the number of nucleon pairs which are able to interact, so the average number of binary inelastic collisions at impact parametr $\mathbf{b}$ is T_{AA} times cross section of nucleon - nucleon collision (*i. e.* the probability of NN interaction).

$$\langle N_{bin}(\mathbf{b}) \rangle = T_{AA}(\mathbf{b}).\sigma_{NN} \tag{4.3}$$

Now we can define the *nuclear modification factor*

$$R_{AA}(p_t, y; \mathbf{b}) = \frac{\text{"real AA collision"}}{\text{"incoherent superposition of NN collisions"}} = \frac{d^2N_{AA}/dydp_T}{T_{AA}(\mathbf{b})d^2N_{NN}/dydp_T} \tag{4.4}$$

which measures the deviation of A+A at impact parametr **b** from an incoherent superposition of nucleon-nucleon collisions [5]. In other words, if the interaction between constituents isn't influenced by the surrounding, then R_{AA} should be one for all p_T. Thus, R_{AA} is the ideal measurable for studying the medium induced changes in jet properties in heavy ion collisions.

Nuclear modification factor can be also defined relative to peripheral collisions:

$$R_{CP} = [\frac{d^2N/p_Tdydp_T/\langle N_{bin}\rangle]^{central}}{d^2N/p_Tdydp_T/\langle N_{bin}\rangle]^{peripheral}} \tag{4.5}$$

4.2 Experimental results

One of the most interesting results from RHIC mesurements is the suppression of high p_T hadrons. This suppression is quantified by above defined nuclear modification factor R_{AA}. *"If the absence of any modification resulting from the "embedding" of elementary collisions in a nuclear collision we expect $R_{AA} \approx 1$ at high p_T"* [2]

R_{AA} dependence on p_T for $\pi^+ + \pi^-$ for two beam energies ($\sqrt{s_{NN}}$ = 62.4 GeV resp. $\sqrt{s_{NN}}$ = 200 GeV) and different centrality ranges is in figure 4 at bottom panels (data are from STAR experiment, however data from all experiments at RHIC are in very good agreement). For $\sqrt{s_{NN}}$ = 200 GeV R_{AA} values are constant for $p_T \gtrsim 4$ GeV/c and approaches 0.2, *i. e.* the value is five time smaller than for binary-scaling expectations. R_{AA} at $\sqrt{s_{NN}}$ = 62.4 GeV has significantly different behavior: R_{AA} isn't constant for high p_T but decreases for $3 \lesssim p_T \lesssim 8.0$ GeV/c.

R_{CP} dependence on p_T, beam energy and centrality for $\pi^+\pi^-$ and p+$\bar{\text{p}}$ is in figure 4 at upper panels. It is clearly seen that there is a significant difference in the p_T dependence between R_{CP} for $\pi^+ + \pi^-$ and R_{CP} for p+$\bar{\text{p}}$ at intermediate p_T. R_{CP} for p+$\bar{\text{p}}$ reaches higher values at its maximum and then has a steeper fall with p_T compared to $\pi^+ + \pi^-$. At high p_T the R_{CP} approach the same values for both mesons and baryons. R_{CP} as a function of centrality decreases with increasing centrality for both $\pi^+ + \pi^-$ and p+$\bar{\text{p}}$. The R_{CP} values at the same centrality are lower for higher beam energy mainly for $p_T \gtrsim 7$ GeV/c, for lower p_T the difference isn't significant.

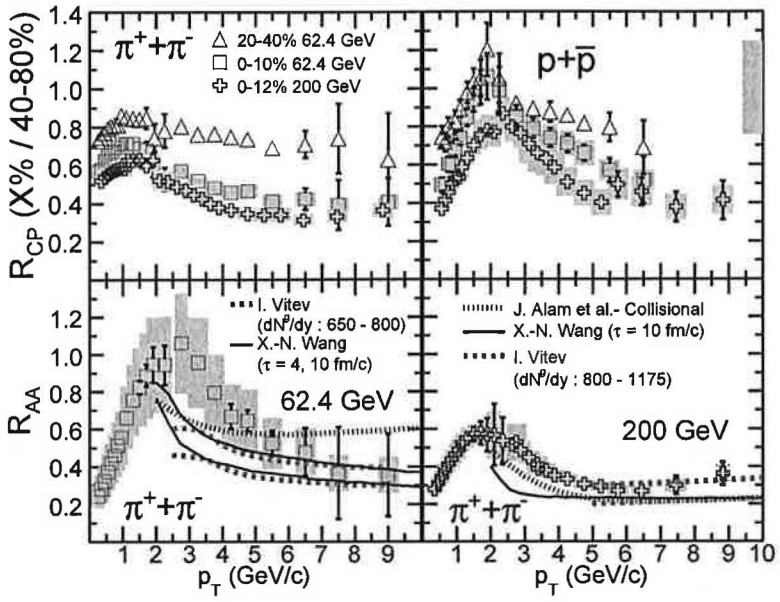

Figure 4.1: Upper panels: R_{CP} dependence on centrality (only at $\sqrt{s_{NN}} =$ 62.4 GeV) and p_T for $\pi^+ + \pi^-$ and p+$\bar{\text{p}}$ at $\sqrt{s_{NN}} = 62.4$ and 200 GeV. Lower panels: R_{AA} dependence for $\pi^+ + \pi^-$ on p_T for two beam energies. Three model predictions are shown. Figure taken from [8]

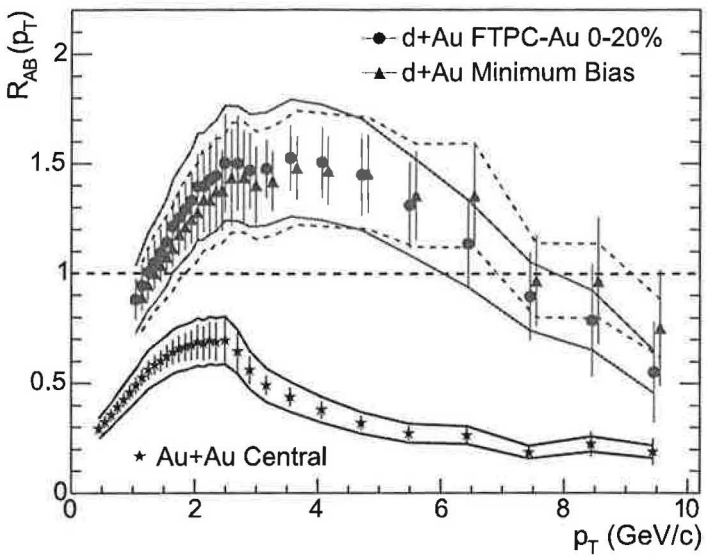

Figure 4.2: R_{dAu} dependence on p_T for minimum bias and central d+Au collisions and $R_{AA}(p_T)$ for central Au+Au collisions. Figure taken from [9]

Figure 5 shows the nuclear modification factor (R_{dAu}) for minimum bias and central d+Au collisions. There is also R_{AA} for central Au+Au collisions. The difference between R_{dAu} for d+Au and R_{AA} for Au+Au collisions is evident: high p_T hadrons for central Au+Au collisions are strongly suppressed by a factor ≈ 5 ($R_{AA} \approx 0.2$ for high p_T) relative to binary scaling expectations whereas in d+Au the suppression is not seen.

4.3 Interpretation

The R_{AA} values for $\sqrt{s_{NN}} = 200$ GeV show strong suppression by a factor $\approx$ 5. This imply the creation of strongly interacting matter, with high transport coefficient $\langle\hat{q}\rangle$ (see equation 1). The $R_{AA} = 0.2$ value is consistent with $\langle\hat{q}\rangle \approx 14$ GeV^2/fm. [5]. The difference between R_{AA} at the two beam energies may be caused by the energy dependence of *"the initial jet spectrum, the parton energy loss and the relative contributions of quark and gluon jets."* [8] Different p_T dependence for baryons vs. mesons may be explained by the difference in quark and gluon energy loss. [8]

The contrast between d+Au and Au+Au collisions in figure 5 indicates and proves that the cause of the strong p_T suppression is associated with the medium produced in Au+Au.

Chapter 5

Dihadron azimuthal correlations

5.1 Introduction

We are considered in interactions where jets are created in pairs. Then the transverse momentum of jets have the same magnitude but opposite direction. If one of the mother-partons traverse significantly longer lenght through the hot and dense medium, the shape of the jet can be modified. This jet is called away-side jet while the jet with unchanged properties is called near-side jet. Full jet reconstruction in Au+Au collisions is inpractical due to overwhelming background of soft particles in the event [5]. Thus, the modification of the jet shape is studied via dihadron azimuthal angle ($\Delta\phi$) correlations.

5.2 Experimental results

Dihadron azimuthal angle correlations express the average number of hadrons (labeled as B) with p_T in chosen range (p_T^B) and at angular distance $\Delta\phi$ from trigger hadron A with p_T^A.

$$Y_{jet} = \frac{1}{N^A}\frac{dN^{AB}}{d\Delta\phi} \tag{5.1}$$

The measured per-trigger yields for p+p and 0-20 % central Au+Au at $\sqrt{s_{NN}}$ = 200 GeV are in figure 6. There are eight panels with different

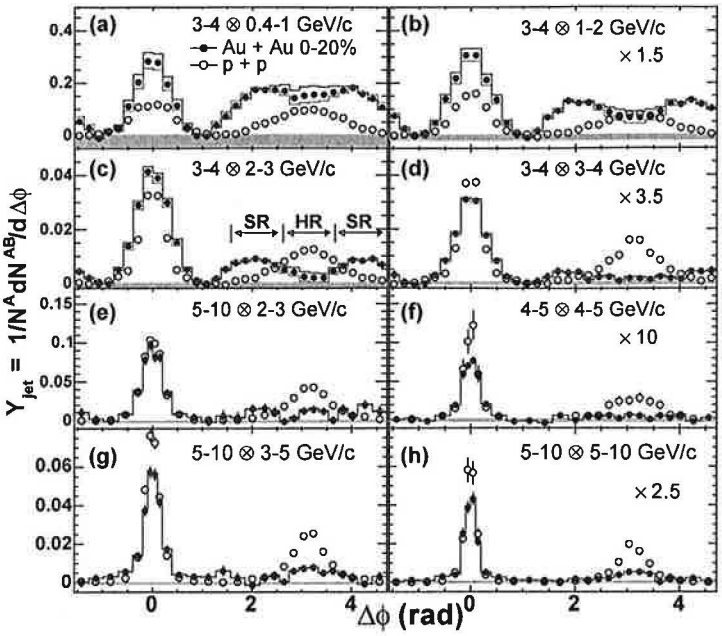

Figure 5.1: Per-trigger yields as a function of $\Delta\phi$ for various trigger and partner p_T ($p_T^A \otimes p_T^B$) in p+p and 0-20 % Au+Au collisions. Arrows in (c) indicate "head" (HR) and "shoulder" (SR) regions.

combinations of p_T^A, p_T^B ranges. The p+p data (open symbols) has Gaussian away-side peak at $\Delta\phi = \pi$ for all p_T^A and p_T^B. The Au+Au data have very different behavior, the shape of the distribution is dependent on p_T^A and p_T^B. For a fixed value of p_T^A, panels (a)-(d) reveal a striking evolution from a broad, roughly flat peak to a local minimum at $\Delta\phi \sim \pi$ with side-peaks at $\Delta\phi \sim \pi \pm 1.1$.[10] The location of side-peaks does not vary with increasing p_T^B and is roughly constant.

For relatively high values of $p_T^A \otimes p_T^B$ (panels (e)-(h)) the away-side jet shape for Au+Au fluently changes to Gaussian peak with similar shape as for p+p but suppressed. It seems that it is caused by bigger suppression of side-peaks at $\Delta\phi \sim \pi \pm 1.1$ relative to that at $\Delta\phi \sim \pi$.

The evolution of the away-side jet shape with p_T leads to separation of the contributions from medium induced components $\Delta\phi \sim \pi \pm 1.1$ and fragmentation component centered at $\Delta\phi \sim \pi$. "A model independent study of these contributions can be made by dividing the away-side jet function

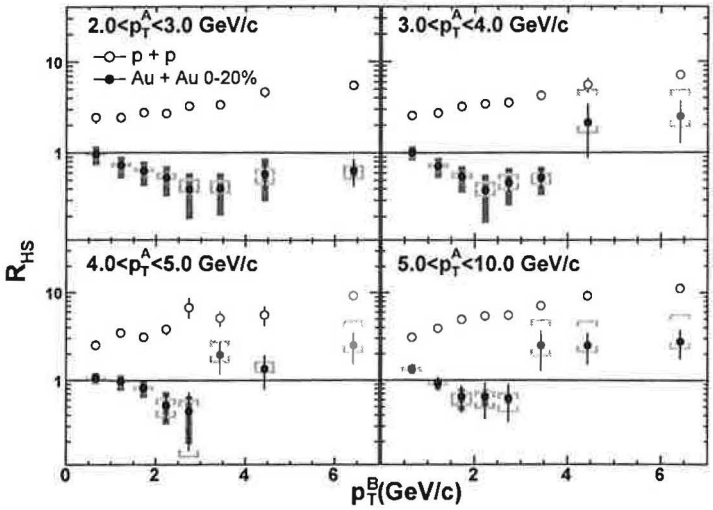

Figure 5.2: R_{HS} versus p_T^B for p+p (opened symbols) and Au+Au at 0-20 % centrality (filled symbols) for four trigger selections. Figure taken from [10]

into equal-sized "head" ($\mid \Delta\phi - \pi \mid < \pi/6$, HR) and "shoulder" ($\pi/6 < \mid \Delta\phi - \pi \mid < \pi/2$, SR) regions." [10] This separation is indicated in panel (c). The relative amplitude of these two regions can be expressed as [10]:

$$R_{\mathrm{HS}} = \frac{\int_{\Delta\phi\in\mathrm{HR}} d\Delta\phi Y_{jet}(\Delta\phi)}{\Delta\phi_{\mathrm{HR}}} \Big/ \frac{\int_{\Delta\phi\in\mathrm{SR}} d\Delta\phi Y_{jet}(\Delta\phi)}{\Delta\phi_{\mathrm{SR}}} \tag{5.2}$$

If the shape of the peak is convex then $R_{\mathrm{HS}} < 1$, if concave then $R_{\mathrm{HS}} > 1$. The dependence of R_{HS} on p_T^B for both p+p and Au+Au is in figure 7. There are four panels with increasing p_T^A ranges. For p+p collisions R_{HS} is always above one and increases with p_T^B. It reflects the narrowing of the peaked jet; jet becomes sharper with more distinctive maximum for higher p_T^B. It is nicely seen on figure 7 at panels (a)-(d). In contrast to p+p the R_{HS} for Au+Au has non-monotonic dependence. The ratios are approximately one for low p_T^B ($p_T^B \lesssim 1$ GeV/c) for all p_T^A ranges. For $1 \lesssim p_T^B \lesssim 3$ GeV/c ratios decrease and are $R_{\mathrm{HS}} < 1$ for all p_T^A. At $p_T^B \lesssim 3$ GeV/c has R_{HS} minimum from which it increases up to one for $2.0 < p_T^A < 3.0$ GeV/c and above one for higher p_T^A ranges.

The results in figure 7 show that relation between p+p and Au+Au yield is suppressed in the head region while in the side region is enhanced. This

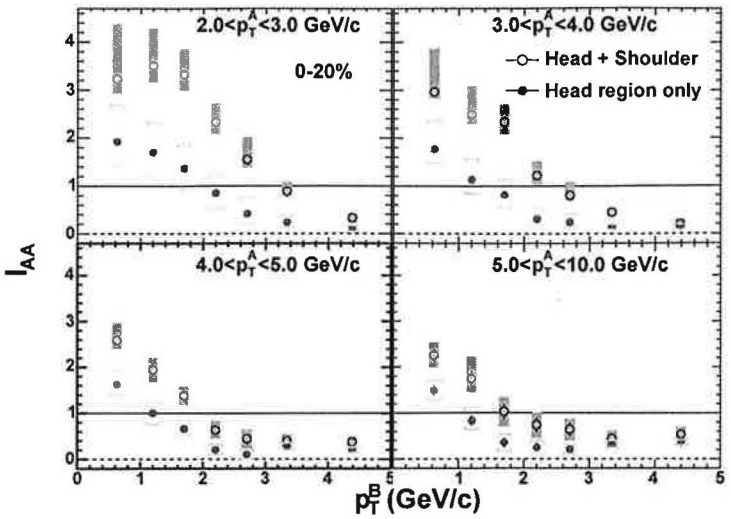

Figure 5.3: I_{AA} versus p_T^B in SR+HR or HR region only for four trigger bins. 0-20 % centrality for Au+Au collisions. Figure taken from [10]

relation is quantified via I_{AA}, the ratio between Au+Au yield Y_{jet}^{Au+Au} and p+p yield Y_{jet}^{p+p} over a $\Delta\phi$ region W (either HR+SR or HR only) [10]

$$I_{AA}^{W} = \int_{\Delta\phi\in W} d\Delta\phi Y_{jet}^{Au+Au} \Big/ \int_{\Delta\phi\in W} d\Delta\phi Y_{jet}^{p+p} \tag{5.3}$$

Figure 8 shows the I_{AA} as a function of p_T^B for both SR+HR (open symbols) and only HR (filled symbols) region in four p_T^A bins. I_{AA} for HR+SR at low p_T^B exceeds unity but is lower for high p_T^A. It decreases with p_T^B and croses one from $p_T^B \sim 2$ GeV/c for high p_T^A to $p_T^B \sim 3.5$ GeV/c for low p_T^A. In other words, for high p_T^A is the enhancement at low p_T^B smaller and suppression at high p_T^B is stronger. The I_{AA} values for HR are lower relative to HR+SR for all $p_T^{A,B}$. With increasing p_T^A the I_{AA} in SR+HR and I_{AA} in HR comes near. For higher p_T^A I_{AA} remains constant at $\sim 0.2 - 0.3$ for $p_T^B \gtrsim 2$ GeV/c.

Another interesting characteristics, which suggest the different origin of the SR and HR yields is dependence of the truncated mean $\langle p_T' \rangle \equiv \langle p_T^B \rangle \,|_{1<p_T^B<5 \text{ GeV/c}} - 1$ GeV/c [10] on the number of participating nucleons N_{part}, *i. e.* on the centrality. $\langle p_T' \rangle$ values are in fig. 9 for HR, SR and near-side region ($|\ \Delta\phi\ | < \pi/3$, NR). $\langle p_T' \rangle$ for NR is very weakly dependent on the centrality. However, the values increase with increasing p_T^A.

Also for SR region $\langle p'_T \rangle$ depends on N_{part} weakly but only for $N_{part} \gtrsim 100$. There is significant increase for $N_{part} \lesssim 100$ of the values. $\langle p'_T \rangle$ values are no dependent on p_T^A. In contrast, yields in the HR are strongly dependent on N_{part}, with increasing N_{part} values of $\langle p'_T \rangle$ significantly decreases.

5.3 Summary

It is evident, that properties of jet, created from mother-parton which traversed through hot and dense QCD matter, are significantly changed. The away-side double-peak structure is interpreted like medium-induced Mach-shock or Cherenkov-like gluon radiation. However, because the maximum of the side-peaks is constant with increasing p_T^B (see figure 6) it disfavors Cherenkov-like radiation.

The evolution of the away-side peak with p_T (*i. e.* the change from double-peak structure to gaussian peak) indicate, that for higher p_T fragmentation component centered at $\Delta\phi \sim \pi$ dominates over medium induced component. This is clearly seen on the figure 7.

I_{AA} ratio for HR region has similar meaning as nuclear modification factor R_{AA} and also its values are consistent with measure of R_{AA}. For $p_T^B \gtrsim 2$ GeV/c yields from Au+Au collisions are suppressed relative to p+p yields at a factor $\backsim 0.2 - 0.3$. I_{AA} values for SR+HR regions are higher than for HR, so it suggests the yield enhancement in SR region. It can be easily explained: if I_{AA} in SR region is higher than in HR then I_{AA} for SR+HR must be higher than only for HR.

The very weak dependence of $\langle p'_T \rangle$ for near side region is consistent with the dominance of jet fragmentation. A $\langle p'_T \rangle$ decrease with N_{part} in HR may reflect the creation of hot and dense matter. For more central collisions the probability of QGP creation is higher what can cause the higher energy loss.

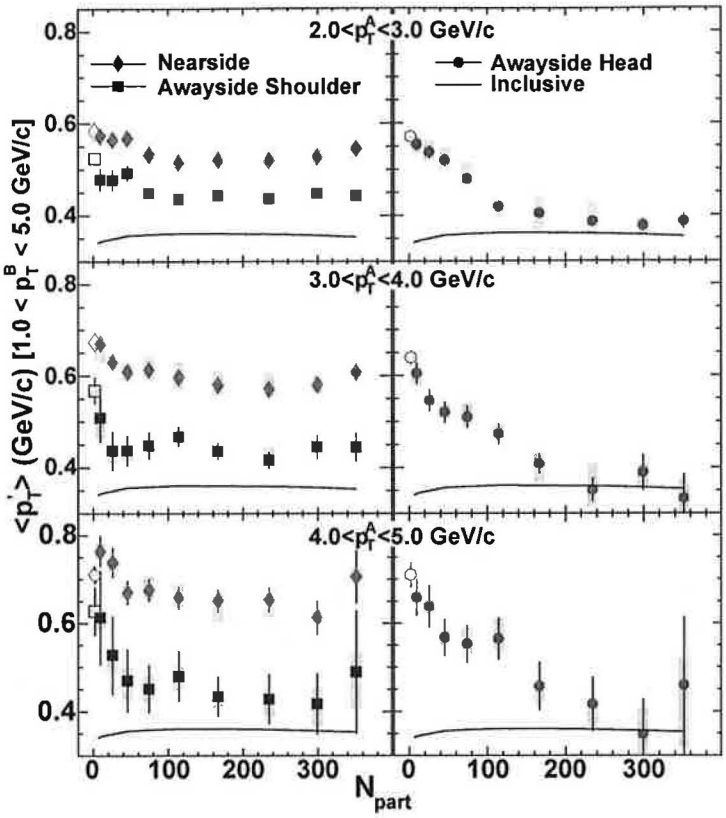

Figure 5.4: $\langle p'_T \rangle$ versus N_{part} in Au+Au collisions in three $\Delta\phi$ regions for three trigger bins. p+p value (open symbols) is also shown. Figure taken from [10]

Chapter 6

Conclusion

Some of the experimental results from RHIC indicating existence of the jet quenching phenomenon are reviewed in this work. Jet quenching was first predicted about 30 years ago but had never been observed before RHIC started its operation program in 2000. This phenomenon is manifested in the suppression of high p_T hadrons production, and in the change of the per-trigger yields distribution. Concrete results taken from experimental papers were presented and discussed for both high p_T hadrons suppression and per-trigger yields but theoretical explanations and interpretations are not mentioned, or are mentioned only particularly due to their difficulty. The general agreement in the interpretations does not exist at all.

Appendix A

RHIC and its experiments

Relativistic Heavy Ion Collider at Brookhaven National Laboratory started its operation program in 2000. Its parametrs are (see also figure 10):

- collider circumference is $\sim$ 3.8 km
- top energy is 200 GeV/nucleon for gold and 250 GeV for protons
- the stored beam lifetime for gold in the energy range of 30 to 100 GeV/nucleon is approximately 10 hours
- designed luminosity for Au+Au at top energy is about $2.10^{26}\mathrm{cm}^{-2}\mathrm{s}^{-1}$ - it corresponds to approximatel 1400 Au+Au minimum bias collisions per second

There are four experiments constructed at RHIC: BRAHMS, PHENIX, PHOBOS and STAR. To cover the broad spectrum of physics topics, every experiment was was designed unlikely to the other.

The BRoad RAnge Magnetic Hadron Spectrometer BRAHMS is designed to measure and identify charged hadrons over wide range of rapidity and transverse momentum. To cover that wide range, it uses two movable spectrometers for the two regions.

The PHENIX experiment is designed to sample rare signals such as J/ψ decaying into muons. Thus it is capable to handle high event rates up to ten times designed luminosity.

The PHOBOS experiment's main goal is to detect as many particles as possible. Another feature is the ability to measure particle with very low momentum.

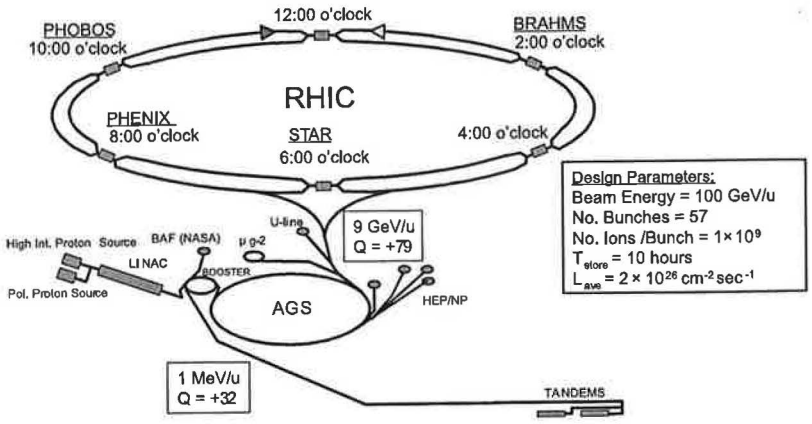

Figure A.1: The Relativistic Heavy Ion Collider comples at Brookhaven National Laboratory

The STAR is a large acceptance detector capable of tracking charged particles and their momenta in the expected high multiplicity enviroment.

Bibliography

[1] J. Adams *et al.* [STAR Collaboration]: Experimental and Theoretical Challenges in the Search for the Quark Gluon Plasma, *arXiv:nucl-ex/0501009*, 2005

[2] I. Arsene *et al.* [Brahms Collaboration]: Quark Gluon Plasma and Color Glass Condensate at RHIC? The perspective from the BRAHMS experiment, *arXiv:nucl-ex/0410020*, 2004

[3] S. S. Adler *et al.* [PHENIX Collaboration]: Formation of dense partonic matter in relativistic nucleus-nucleus collisions at RHIC, *arXiv:nucl-ex/041003*, 2005

[4] A Peshier: Collisional jet quenching becomes probable, *arXiv:hep-ph/0607299*, 2006

[5] David d'Enterria: Jet quenching: RHIC results and phenomenology, *arXiv:nucl-ex/0510062*, 2005

[6] B. B. Back *et al.* [PHOBOS Collaboration]: The PHOBOS Perspective on Discoveries at RHIC, *arXiv:nucl-ex/0410022*, 2005

[7] I. P. Lokhtin, A. M. Snigirev: Nuclear geometry of jet quenching, *arXiv:hep-ph/0004176*, 2000

[8] B. I. Abelev *et al.* [STAR Collaboration]: Energy dependence of $\pi^{\pm}$, p and $\bar{\text{p}}$ transverse momentum spectra for Au+Au collisions at $\sqrt{s_{NN}} =$ 62.4 and 200 GeV, *arXiv:nucl-ex/0703040*, 2007

[9] J. Adams *et al.* [STAR Collaboration]: Evidence from d+Au measurements for final-state suppression of high p_T hadrons in Au+Au collisions at RHIC, *arXiv:nucl-ex/0306024*, 2003

[10] A. Adare *et al.* [PHENIX Collaboration]: Transverse momentum and centrality dependence of dihadron correlations in Au+Au collisions at $\sqrt{s_{NN}} = 200$ GeV: Jet-quenching and the response of partonic matter, *arXiv:0705.3238*, 2007